Philosophical Magazine, 2013
Vol. 93, No. 22, 3012–3028, http://dx.doi.org/10.1080/14786435.2013.799788

Taylor & Francis
Taylor & Francis Group

Spontaneous athermal cross-slip nucleation at screw dislocation intersections in FCC metals and $L1_2$ intermetallics investigated via atomistic simulations

S.I. Rao[a]*, D.M. Dimiduk[b], J.A. El-Awady[c], T.A. Parthasarathy[a], M.D. Uchic[b] and C. Woodward[b]

[a]*UES, Inc., 4401 Dayton-Xenia Rd, Dayton, OH 45432-1894, US;* [b]*Air Force Research Laboratory, Materials and Manufacturing Directorate, AFRL/RXCM, Wright-Patterson AFB, Dayton, OH 45433-7817, US;* [c]*Department of Mechanical Engineering, Johns Hopkins University, Baltimore, MD 21218, US*

(*Received 11 January 2013; final version received 23 April 2013*)

In this manuscript, we extend on our prior work to show that under certain conditions cross-slip nucleation is athermal and spontaneous with zero activation energy in FCC elemental metals such as Ni and Cu, and $L1_2$ intermetallic compounds such as Ni_3Al. Using atomistic simulations (molecular statics), we show that spontaneous cross-slip occurs at mildly repulsive intersections. Further, the local Shockley partial dislocation interactions at such repulsive intersections are found to be attractive leading to junction formation. The line orientation of the intersecting dislocation determines whether the spontaneous cross-slip nucleation occurs from either the glide plane to the cross-slip plane or vice versa. Collectively, these results suggest that cross-slip should be preferentially observed at selected screw dislocation intersections in FCC-derviative metals and alloys.

Keywords: cross-slip; dislocation intersections; atomistic simulations; nickel; copper

1. Introduction

Cross-slip of screw dislocations is an elementary thermally-activated mechanism that is ubiquitous in plastic deformation and is recognized as the most important single process underlying complex spatiotemporal developments in dislocation microstructure. The phenomenon leads to the onset of a fully-plastic flow via dislocation multiplication, strain hardening, dislocation pattern formation and dynamic recovery [5,6]. The early work of Friedel and Escaig remains the most widely cited and used model for cross-slip [7–11], however, this model poses several difficulties with respect to quantitative simulations as detailed in our prior works [1–4]. Advances in atomistic simulations make it possible to gain insights into the cross-slip process and may serve to inform mesoscale simulations to accurately capture the atomic-level physics of dislocation process.

*Corresponding author. Email: Satish.Rao@wpafb.af.mil

Previously, using atomistic simulations (molecular statics) with embedded atom method interatomic potentials, we evaluated the activation barrier for a screw-character dislocation to transform from fully residing on the glide (GL) plane to fully residing on the cross-slip plane, when intersecting a selected forest dislocation. For those simulations the screw-character dislocation was intersecting a mildly-attractive 120° forest dislocation forming either GL, Lomer-Cottrell (LC) or Hirth locks in both Ni and Cu [1,2]. The activation energies were computed using two different techniques: (a) determining equilibrium configurations (energies) when varying pure tensile or compressive stresses were applied along the [1 1 1] direction on the partially cross-slipped state and (b) the classical nudged elastic band method. The cross-slip activation energies at the intersections were found to be a factor of 3–20 lower than the energy for cross slip in the perfect crystal via constriction formation and the Friedel–Escaig mechanism (FE mechanism). This intersection cross-slip mechanism seems to provide a better physical basis for cross-slip since no ad hoc assumptions about dislocation obstacles are required; thus warranting further investigation.

In this work, the Burgers vector b, of the intersecting dislocation corresponding to LC, and GL formation are reversed, and cross-slip nucleation is examined at what become mildly-repulsive intersections, for atomistic potentials corresponding to FCC Ni, Cu and $L1_2$ Ni_3Al. The simulations show that cross-slip nucleation at these intersections is spontaneous and athermal, having zero cross-slip activation energy for all three materials. The remainder of this paper is organized as follows. Section 2 describes the simulation technique, the interatomic potentials used in the simulations, and it briefly describes the method used to both analyse and visualize the dislocation core structures. Section 3 contains the results of the simulations, Section 4 presents a brief discussion of the results, and Section 5 gives a summary of the results.

2. Simulation technique

The atomistic simulations described here employed the three-dimensional (3-D) parallel molecular dynamics (MD) code, LAMMPS [12], developed at Sandia National Laboratory. The simulation cell is a rectangular parallelepiped having the x-axis oriented along the $[1\,\bar{1}\,0]$ direction, y-axis along the $[1\,1\,\bar{2}]$ direction, and the z-axis along [1 1 1]. The dimensions of the simulation cells vary from 62 to 124 nm along the x-axis and from 32 to 124 nm along both the y- and z-axes, corresponding to simulation cells that contain between 5 and 170 million atoms. A $\frac{1}{2}[1\,\bar{1}\,0]$ screw-character dislocation dissociated into two Shockley partials separated by $5b$ (where $b = |\mathbf{b}|$) on the (1 1 1) glide plane is placed at a pre-determined distance, ranging from 0 to 100 Å, away from the middle of the simulation cell along the $[1\,1\,\bar{2}]$ direction using its anisotropic elastic displacement field [13]. In a few simulations, the screw dislocation was inserted as two Shockley partials separated by $5b$ on the $(1\,1\,\bar{1})$ cross-slip plane. An intersecting dislocation, with Burgers vector $\frac{1}{2}[1\,0\,\bar{1}]$ or $\frac{1}{2}[0\,\bar{1}\,\bar{1}]$ was also inserted in the middle of the simulation cell using its anisotropic elastic displacement field. The line orientation of the intersecting dislocation was one of the following: $\langle 0\,\bar{1}\,\bar{1}\rangle$, $\langle 1\,\bar{1}\,\bar{2}\rangle$ or $\langle 2\,1\,\bar{1}\rangle$. For simplicity, fixed boundary conditions were applied along all three directions and energy minimization was performed using the conjugate gradient technique. In some cases,

MD constant NVT (number of atoms, N, volume, V and temperature T) relaxations were performed on the initial atomic positions at a low temperature of 0.1 K.

2.1. *Interatomic potentials*

The embedded atom potentials used for the simulations are those developed for FCC Ni by Angelo, Moody and Baskes [13] based on the Voter and Chen format (Angelo), Ni potentials developed based on the Voter and Chen format which Rao et al. used within their FE mechanism cross-slip simulations, 'vni' and 'vnih' [14], as well as a Ni potential developed by Mishin et al. [15]. The embedded atom potential used for the simulations of Cu was that developed by Mishin et al. [16]. Table 1 gives the lattice parameter, cohesive energy, elastic constants and stacking fault energy for each of the potentials [1]. The four Ni potentials used in the simulations give almost identical elastic constants, cohesive energies and lattice parameters (close to experimental values), whereas the stacking fault energy given by the potentials varies from 59 (vni), 89 (Angelo), 120 (vnih) to 134 mJ/m^2 (Mishin). The Shockley partial spacing width, d, for the screw dislocation varies from $d/b = 4$–5 for potentials vnih and Mishin, to $d/b = 7$ for the vni potential, where b is the magnitude of the Burgers vector of the screw dislocation. The Angelo potential gives a d/b ratio of 6. Since the experimentally determined stacking fault energy of Ni is close to 120 mJ/m^2, results from potentials vnih and Mishin should be representative of Ni. In addition to Mishin and vnih potentials, results from Angelo and vni potentials are also given to determine the effect of stacking fault energy or 'd/b' ratio on the spontaneous cross-slip process. The EAM potential developed for Cu by Mishin et al. [16] gives the lattice parameter, cohesive energy, elastic constants and stacking fault energy which are very nearly equal to the experimental values and the results from this potential should be a representative of Cu. The Mishin potential gives a d/b ratio of 6 for Cu.

For $L1_2$ Ni_3Al we use the Angelo potential [13]. The various planar fault energies given by the Angelo, Mishin1, Mishin2 and Voter potentials for $L1_2$ Ni_3Al are given in Table 2 [4]. The activation energy for screw dislocation cross slip in isolation via the PPV (Paidar–Pope–Vitek) mechanism in $L1_2$ Ni_3Al has been estimated to be 2.49, 0.96 and 0.20 eV, respectively with the Angelo, Mishin1 and Mishin2 potentials [4]. Therefore, to check whether there is spontaneous screw dislocation cross-slip at mildly repulsive intersections in $L1_2$ Ni_3Al, it was decided to use the Angelo potential, which gives the maximum activation energy for screw dislocation cross-slip in isolation.

Table 1. Lattice constants, a_o, cohesive energies, E_c, elastic constants, C_{11}, C_{12} and C_{44}, stacking fault energies, γ, and Shockley partial splitting of the screw dislocation, d/b, given by the four Ni potentials, Angelo, vni, vnih and Mishin and the Cu Mishin potential.

	Angelo	vni	vnih	Mishin (Ni)	Mishin (Cu)
a_0 (A)	3.52	3.52	3.52568	3.52	3.615
E_c (eV)	−4.45	−4.45	−4.4346	−4.45	−3.54
C_{11} ($\times 10^{11}$ N/m^2)	2.464	2.44	2.422	2.413	1.699
C_{12} ($\times 10^{11}$ N/m^2)	1.473	1.49	1.472	1.508	1.226
C_{44} ($\times 10^{11}$ N/m^2)	1.248	1.25	1.185	1.273	0.762
γ (mJ/m^2)	89	59	119	134	44
d/b	6	7	4–5	4–5	6

Table 2. Lattice Parameters, a_o, Cohesive energies, E_c, Elastic constants C_{11}, C_{12} and C_{44}, Planar Fault energies, γ_{111}, γ_{001}, γ_{csf}, γ_{sisf}, γ_{csf}-$0.5\gamma_{111}$ and the screw superdislocation superpartial core widths, d/b, given by four different EAM potentials for $L1_2$ Ni_3Al, Moody, Mishin1, Mishin2 and Voter.

	Moody	Mishin1	Mishin2	Voter
a_0, A	3.567	3.571	3.533	3.567
E_c, eV	4.598	4.626	4.632	4.600
C_{11} ($\times 10^{11}$ N/m^2)	2.558	2.360	2.382	2.460
C_{12} ($\times 10^{11}$ N/m^2)	1.352	1.490	1.664	1.370
C_{44} ($\times 10^{11}$ N/m^2)	1.242	1.271	1.302	1.230
γ_{111} (mJ/m^2)	202	252	180	142
γ_{001} (mJ/m^2)	129	80	20	83
γ_{csf} (mJ/m^2)	164	202	228	121
γ_{sisf} (mJ/m^2)	5	51	21	13
$\gamma_{csf} - 0.5\gamma_{111}$ (mJ/m^2)	63	76	138	50
d/b	6	4	2	7

2.2. *Depiction of the core structures*

For the depiction of the core structures, we use the method developed by Stukowski and Albe [17] which computes dislocation line representations and their associated Burgers vectors from 3-D atomistic simulations. It is based on a fully automated Burgers circuit analysis, which locates dislocation cores and determines their Burgers vector. The transition from the atomistic system to a discrete dislocation representation is achieved through a subsequent vectorization step. Sophisticated information, including dislocation reactions and junctions can be obtained from this analysis.

3. Results

3.1. $b = \frac{1}{2}[1\,0\,\bar{1}]$ *dislocations in FCC Ni and Cu*

3.1.1. *Molecular statics simulations*

Figure 1 shows a dislocation line representation of the initial configuration as well as the final relaxed configuration (conjugate gradient technique) at a 120° mildly-repulsive screw dislocation intersection in FCC Ni, obtained using the Mishin potential for Ni [15]. The screw dislocation had a $\frac{1}{2}[1\,\bar{1}\,0]$ Burgers vector, $\langle 1\,\bar{1}\,0\rangle$ line direction and was introduced as the two Shockley partials separated by $5b$ along the $[1\,1\,\bar{2}]$ direction on the $(1\,1\,1)$ glide plane. The center of the dislocation was displaced by $2a[1\,1\,\bar{2}]$ along the $[1\,1\,\bar{2}]$ direction on the $(1\,1\,1)$ glide plane, where a is the lattice parameter. The leading Shockley partial had a Burgers vector of $1/6[1\,\bar{2}\,1]$ and the trailing Shockley partial had a Burgers vector of $1/6[2\,\bar{1}\,\bar{1}]$. The intersecting dislocation had a Burgers vector of $\frac{1}{2}[1\,0\,\bar{1}]$ and a line direction of $\langle 0\,\bar{1}\,\bar{1}\rangle$ and was introduced at the center of the simulation cell using its anisotropic elasticity displacement field. The glide plane of the intersecting dislocation was $(1\,\bar{1}\,1)$. This configuration is identical to the 120° mildly attractive screw dislocation intersection considered in [1] forming GL excepting that the Burgers vector of the intersecting dislocation is reversed. In the final relaxed configuration, it is seen that the screw dislocation has spontaneously cross-slipped onto the $(1\,1\,\bar{1})$ cross-slip plane on one side of the intersection forming a partially cross-slipped

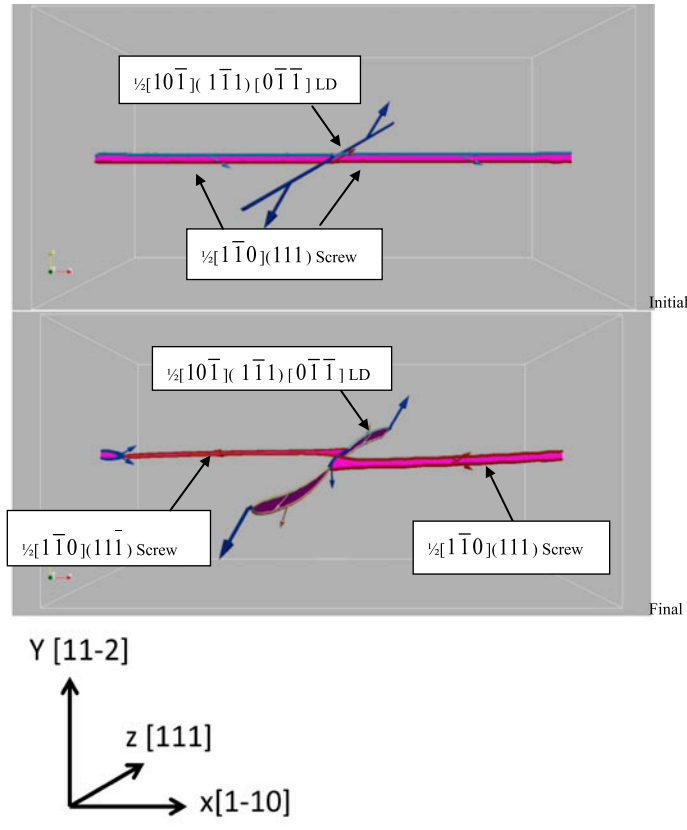

Figure 1. (colour online) A dislocation line representation of the initial and final relaxed atomic positions at a mildly repulsive 120° screw dislocation intersection in FCC Ni obtained using the Mishin potential. For all figures depicting dislocation line representations the dislocation lines are colored according to their length and, the colored arrows represent Burgers vector magnitude and direction. Note that the screw dislocation has spontaneously cross-slipped to form the partially cross-slipped state in the final configuration.

configuration at the intersection. This partially cross-slipped configuration is similar to the partially cross-slipped configuration obtained for the mildly attractive 120° intersection in [1], excepting that cross-slip is spontaneous in this case and the cross-slipped portion is on the opposite side of the intersection. To verify that cross-slip is indeed spontaneous, the initial conditions to the simulations were modified as follows. The screw dislocation (introduced as two Shockley partials) was allowed to completely relax before introducing the intersecting dislocation using its anisotropic elasticity displacement field. Once again, the screw dislocation spontaneously cross-slipped and formed the partially cross-slipped configuration, confirming that cross-slip is indeed spontaneous at this mildly-repulsive 120° intersection having zero activation energy. Note also that the fully glide-plane configuration for the screw dislocation at this mildly-repulsive intersection is unstable, as there are two attractive Shockley partial interactions. First, the constricted 120° intersecting dislocation reacts with one of the Shockley partials of

the screw dislocation having $1/6[2\,\bar{1}\,\bar{1}]$ Burgers vector on the $(1\,1\,1)$ glide plane to form the $1/6\langle 1\,1\,\bar{2}\rangle$ Burgers vector as follows:

$$1/2[1\,0\,\bar{1}] + 1/6[\bar{2}\,1\,1] = 1/6[1\,1\,\bar{2}]$$

Second, one of the Shockley partials of the intersecting dislocation having $1/6[1\,\bar{1}\,\bar{2}]$ Burgers vector reacts with one of the Shockley partials of the screw dislocation on the cross-slip plane having $1/6[\bar{1}\,2\,1]$ Burgers vector to form the $1/6[0\,1\,\bar{1}]$ Burgers vector as follows:

$$1/6[1\,\bar{1}\,\bar{2}] + 1/6[\bar{1}\,2\,1] = 1/6[0\,1\,\bar{1}]$$

Similar spontaneous cross-slip was observed at this intersection even for initial stand-off distances of the screw dislocation along the $[1\,1\,\bar{2}]$ direction on the $(1\,1\,1)$ plane of up to 100 Å. Such large stand-off distance simulations were performed with a 170 million atom cell, corresponding to x, y and z cell dimensions of 124 nm. Therefore, even though the long-range interaction between the intersecting and screw dislocation is mildly repulsive, the short-range Shockley interactions between the two dislocations are attractive, leading to junction formation and Shockley reactions. This suggests that the initial conditions to the simulations discussed here, placing the two dislocations with a certain stand-off distance, is realistic and minimal stresses are required for the screw dislocation to interact with the intersecting dislocation. Similar molecular statics simulations were performed using the other two Ni potentials, 'vnih' and 'Moody' as well as the Cu Mishin potential. Figures 2–4 show a dislocation line representation of the final relaxed configuration obtained with these potentials. In all cases, the screw dislocation has spontaneously cross-slipped to form the partially cross-slipped configuration, similar to the Ni Mishin potential results.

3.1.2. *MD simulations*

To determine the pathway that the screw dislocation takes to spontaneously cross-slip at the mildly-repulsive 120° intersection, molecular dynamics constant NVT simulations at a low temperature of 0.1 K were performed on the initial conditions shown in Figure 1 with the Ni Mishin potential. Figure 5 shows the dislocation line representation of the atomic positions in the simulation cell at timesteps of 3500 and 4500 femtoseconds. Note that in Figure 5, the direction of x-axis is reversed with respect to Figures 1–4. At 3500 femtoseconds, a small length of the screw dislocation at the intersection has completely constricted to form the full $\frac{1}{2}[1\,\bar{1}\,0]$ Burgers vector. At 4500 femtoseconds, the fully-constricted screw dislocation at the intersection has re-dissociated on the cross-slip plane resulting in the screw dislocation spontaneously forming the partially cross-slipped configuration at the intersection. These results indicate that the mechanism of the spontaneous cross-slip at the mildly-repulsive 120° intersection is related to the FE mechanism, similar to that in perfect crystals [14]. Seemingly, the principal role of the intersecting dislocation is to provide an obstacle that enables constriction formation. However, the activation energy is zero at this intersection, a dramatic reduction

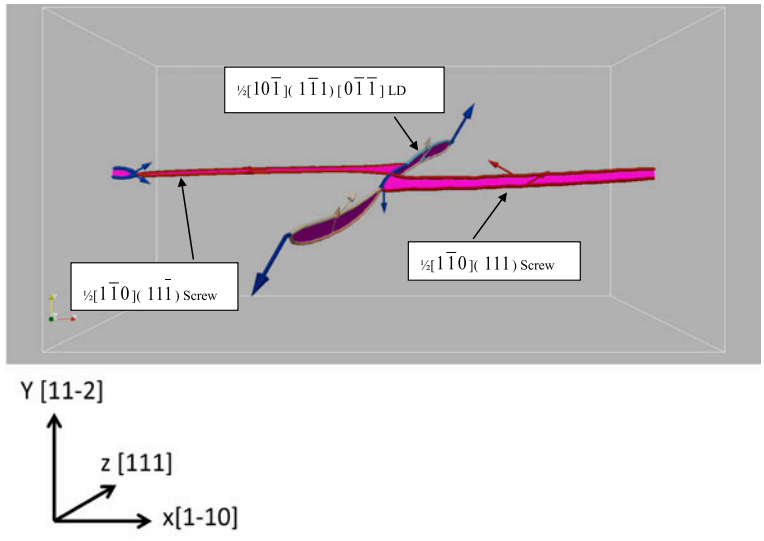

Figure 2. (colour online) A dislocation line representation of the final relaxed atomic positions at a mildly repulsive 120° screw dislocation intersection (as in Figure 1) obtained using the Angelo potential. Note the partially cross-slipped state of the screw dislocation.

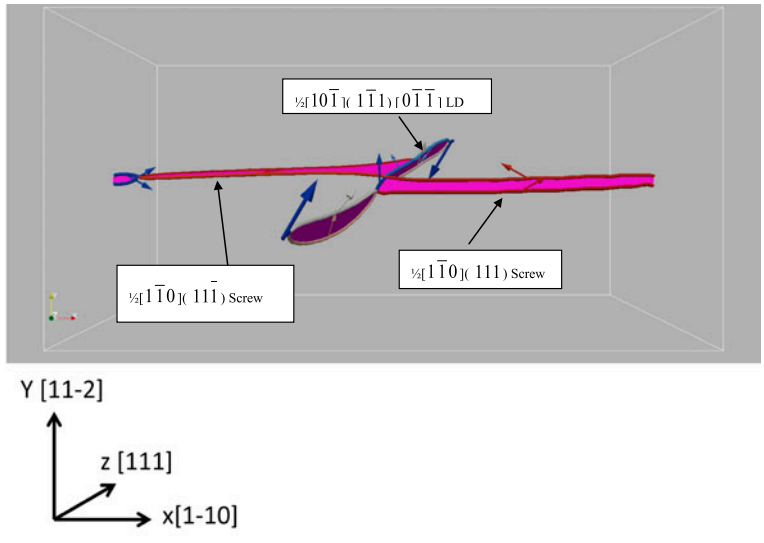

Figure 3. (colour online) A dislocation line representation of the final relaxed atomic positions at a mildly repulsive 120° screw dislocation intersection in FCC Ni obtained using the potential 'vnih'. Note the partially cross-slipped state of the screw dislocation.

compared to the high value of 1.85 eV for cross slip via the FE mechanism away from intersections (Ni Mishin potential) [2]. This effect is most probably due to the Escaig stresses from the 120° intersecting dislocation acting on the Shockley partials of the screw dislocation at the intersection. Similar molecular dynamics simulations were

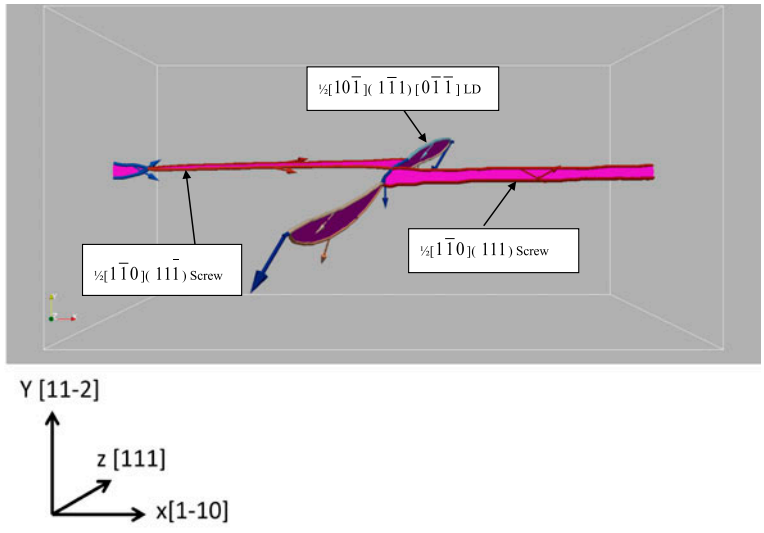

Figure 4. (colour online) A dislocation line representation of the final relaxed atomic positions at a mildly repulsive 120° screw dislocation intersection in FCC Cu obtained using the Cu Mishin potential. Note the partially cross-slipped state of the screw dislocation.

performed with the other potentials. Potentials 'vni' and 'vnih', as well as the Cu Mishin potential show the FE mechanism for spontaneous cross slip at the mildly repulsive intersection, similar to the Ni Mishin potential. However, the Ni 'Angelo' potential shows a different mechanism for the cross-slip at the intersection. In this case, the mechanism for spontaneous cross-slip at the intersection is similar to the 'Fleischer Mechanism' of cross-slip postulated for the screw dislocation in isolation [18]. Figure 6 gives a dislocation line representation of the molecular dynamics simulation results obtained with the Angelo potential at timesteps of 2500 and 3250 femtoseconds. In Figure 6, similar to Figure 5, the direction of *x*-axis is reversed with respect to Figures 1–4. At 2500 femtoseconds, one of the Shockley partials of the screw dislocation on the (1 1 1) glide plane with 1/6[2 $\bar{1}$ $\bar{1}$] Burgers vector has dissociated into a stair-rod dislocation with 1/6[1 1 0] Burgers vector and a Shockley partial on the cross-slip plane with 1/6[1 $\bar{2}$ $\bar{1}$] Burgers vector. Similarly, a Shockley partial of the intersecting dislocation having 1/6[1 $\bar{1}$ $\bar{2}$] Burgers vector has dissociated into a stair-rod dislocation having 1/6[0 1 $\bar{1}$] Burgers vector and a Shockley partial having 1/6[1 $\bar{2}$ $\bar{1}$] Burgers vector. The line direction of the 1/6[1 $\bar{2}$ $\bar{1}$] Shockley dislocations formed from the screw and intersecting dislocations are opposite in character locally and annihilate each other, making these two stair-rod dislocation reactions energetically favourable. Finally, at time = 3250 femtoseconds, the 1/6[1 1 0] stair-rod dislocation has an attractive interaction with the 1/6[1 $\bar{2}$ 1] Shockley partial of the screw dislocation on the (1 1 1) glide plane to form the other Shockley partial of the screw dislocation on the cross-slip plane with Burgers vector 1/6[2 $\bar{1}$ 1], thereby completing the cross-slip process. This suggests that the mechanism of spontaneous cross-slip at the 120° mildly-repulsive screw dislocation intersection is dependent on the details of the atomic interactions, with the most likely process being the FE mechanism.

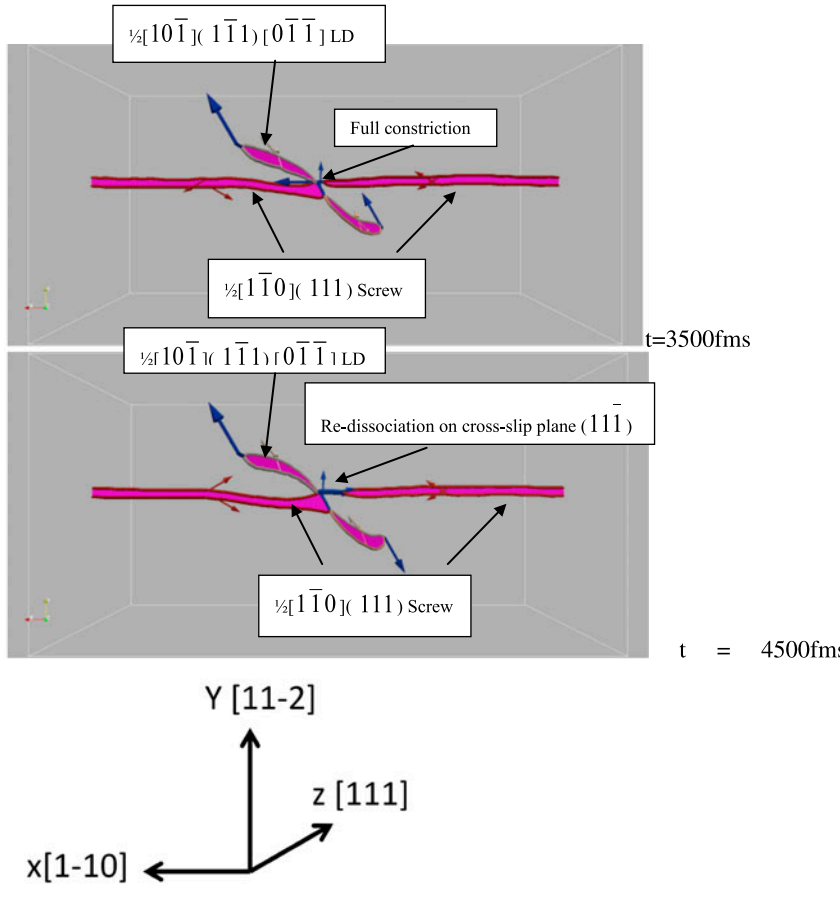

Figure 5. (colour online) A dislocation line representation of the atomic positions of a molecular dynamics simulation (0.1 K) at a mildly repulsive 120° screw dislocation intersection in FCC Ni obtained using the Mishin potential at $t = 3500$ and 4500 femtoseconds. At $t = 3500$ femtoseconds, the screw dislocation has completely constricted over a small length at the intersection. At $t = 4500$ femtoseconds, the constricted screw has redissociated on the cross-slip plane to form the partially cross-slipped state.

3.2. $b = ½[0\,\bar{1}\,\bar{1}]$ *dislocations in FCC Ni*

Figure 7 is a dislocation line representation of the final relaxed configuration (conjugate gradient technique) at a mildly-repulsive screw dislocation intersection in FCC Ni, obtained using the Mishin potential for Ni [15]. In this case, the intersecting dislocation had a Burgers vector of ½[0 $\bar{1}$ $\bar{1}$] (the reverse Burgers vector forms a LC lock at the intersection) and a line direction of $\langle 1\,\bar{1}\,2\rangle$ and was introduced at the center of the simulation cell using its anisotropic elasticity displacement field. The glide plane of the intersecting dislocation was (1 $\bar{1}$ 1). In the final relaxed configuration, it is seen that the screw dislocation has spontaneously cross-slipped onto the (1 1 $\bar{1}$) cross-slip plane on one side of the intersection forming a partially cross-slipped configuration at the intersection. As for the 1/2[1 0 $\bar{1}$] Burgers vector of the intersecting dislocation, there are

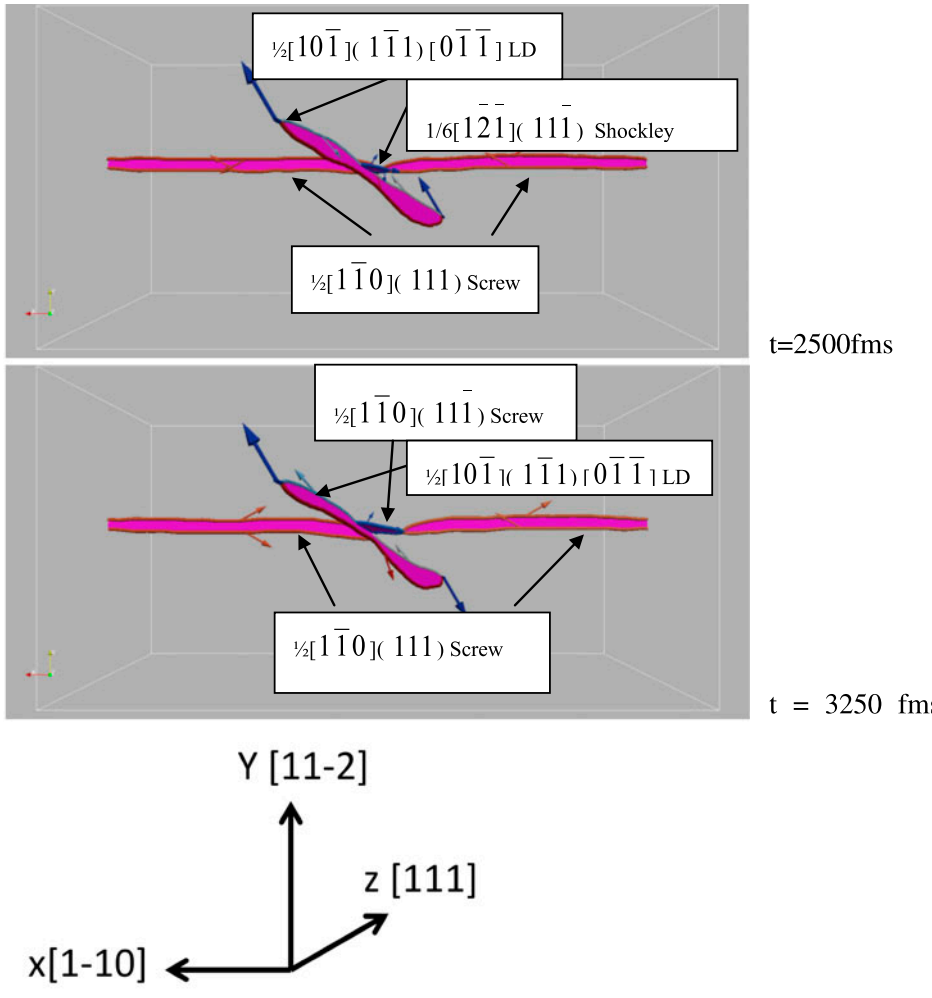

Figure 6. (colour online) A dislocation line representation of the atomic positions of a molecular dynamics simulation (0.1 K) at a mildly repulsive 120° screw dislocation intersection in FCC Ni obtained using the Angelo potential at $t = 2500$ and 3250 femtoseconds. The Angelo potential shows a Fleischer type mechanism of spontaneous cross-slip at the intersection.

two attractive Shockley partial interactions at this intersection: first, the constricted 120° intersecting dislocation reacts with one of the Shockley partials of the screw dislocation with $1/6[\bar{1}\,2\,1]$ Burgers vector on the $(1\,1\,\bar{1})$ cross-slip plane to form the $1/6\langle\bar{1}\,\bar{1}\,2\rangle$ Burgers vector as follows:

$$1/2[0\,\bar{1}\,\bar{1}] + 1/6[\bar{1}\,2\,1] = 1/6[\bar{1}\,\bar{1}\,\bar{2}]$$

Second, one of the Shockley partials of the intersecting dislocation with $1/6[1\,\bar{1}\,\bar{2}]$ Burgers vector reacts with one of the Shockley partials of the screw dislocation on the

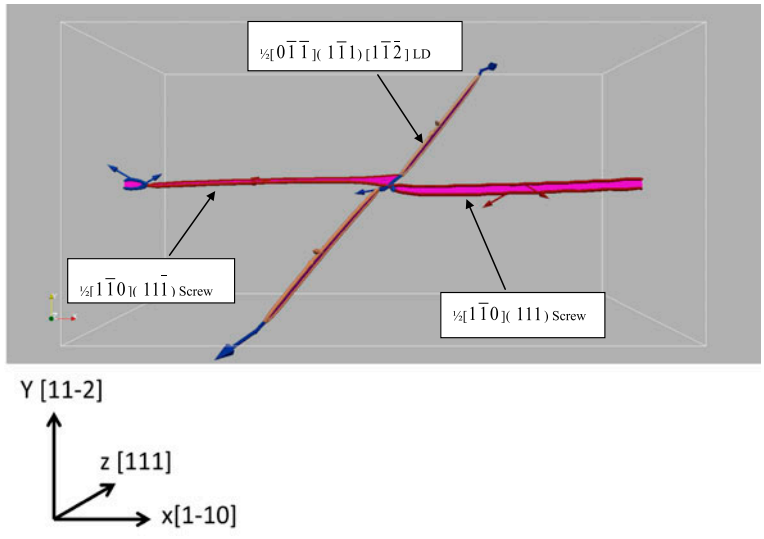

Figure 7. (colour online) A dislocation line representation of the final relaxed atomic positions at a mildly repulsive screw dislocation intersection in FCC Ni obtained using the Mishin potential. Note the partially cross-slipped state of the screw dislocation.

(1 1 1) glide plane having $1/6[\bar{2}\,1\,1]$ Burgers vector to form the $1/6[\bar{1}\,0\,\bar{1}]$ Burgers vector as follows:

$$1/6[1\,\bar{1}\,\bar{2}] + 1/6[\bar{2}\,1\,1] = 1/6[\bar{1}\,0\,\bar{1}]$$

Figure 8 is also a dislocation line representation of the final relaxed configuration (conjugate gradient technique) at a mildly repulsive screw-dislocation intersection in FCC Ni, obtained using the Mishin potential for Ni [15]. The screw dislocation was identical to Figure 7 excepting that it was introduced initially as two Shockley partials separated by 5*b* on the $(1\,1\,\bar{1})$ cross-slip plane. The intersecting dislocation in Figure 8 had a $\frac{1}{2}[0\,\bar{1}\,\bar{1}]$ Burgers vector and a line direction of $[2\,1\,\bar{1}]$. In this case, the screw dislocation spontaneously cross-slips from the cross-slip plane to the (1 1 1) glide plane to form the partially cross-slipped configuration. Several such simulations for varying line orientations of the repulsive intersecting dislocation were performed to determine the spontaneous cross-slip map for the screw dislocation and is shown in Figure 9. In Figure 9, for line orientations of the repulsive intersecting dislocation in the upper quadrant, the screw dislocation spontaneously cross slips from the (1 1 1) glide plane to the $(1\,1\,\bar{1})$ cross-slip plane, whereas for the lower quadrant the spontaneous cross-slip tendency is reversed (i.e.) the screw dislocation spontaneously cross-slips from the $(1\,1\,\bar{1})$ cross-slip plane to the (1 1 1) glide plane. The common line direction between the $(1\,1\,\bar{1})$ cross-slip plane and the glide plane of the intersecting dislocation, $(1\,\bar{1}\,1)$, lies in the upper quadrant whereas the common line direction between the (1 1 1) glide plane and the $(1\,\bar{1}\,1)$ plane lies in the lower quadrant. The strength of junctions formed at the intersection are higher, lower is the angle between the line direction of the intersect-

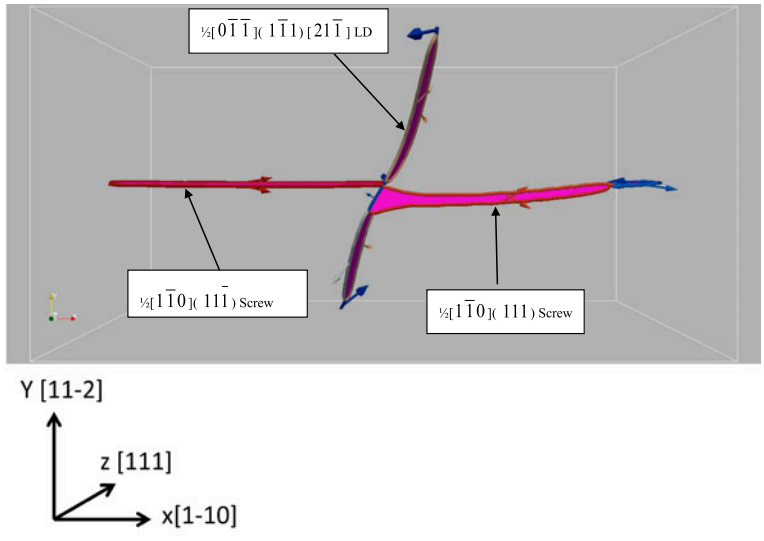

Figure 8. (colour online) A dislocation line representation of the final relaxed atomic positions at a mildly repulsive screw dislocation intersection in FCC Ni obtained using the Mishin potential. The screw dislocation has spontaneously cross-slipped from the (1 1 1̄) cross-slip plane to the (1 1 1) glide plane to form the partially cross-slipped state.

ing dislocation and this common line direction. Therefore, it is postulated, that the screw dislocation cross slips onto a plane where the strength of the junctions formed is higher. This spontaneous cross-slip map is similar for both the ½[1 0 1̄] and ½[0 1̄ 1̄] Burgers vectors of the intersecting dislocation.

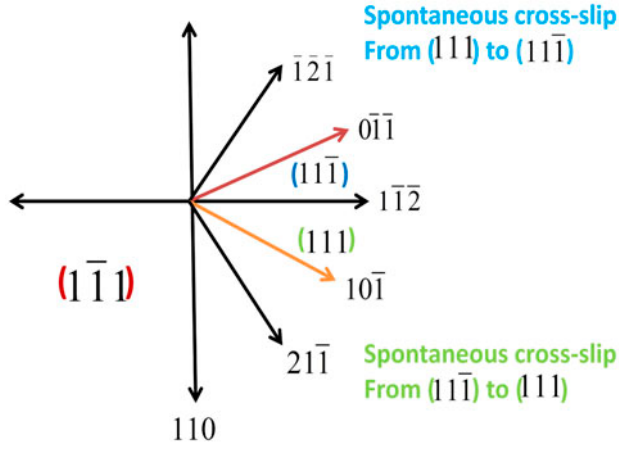

Figure 9. (colour online) A spontaneous cross-slip map for a mildly repulsive screw dislocation intersection in FCC Ni. The screw dislocation had a ½[1 1̄ 0] Burgers vector and the intersecting dislocation had a ½[0 1̄ 1̄] Burgers vector. The line directions of the intersecting dislocation on the (1 1̄ 1) plane are shown in two quadrants along with the direction of spontaneous cross-slip of the screw dislocation for both quadrants.

3.3. $b = [1\,0\,\bar{1}]$ *Molecular statics simulations of* $L1_2$ Ni_3Al

Figure 10 is a dislocation line representation of the initial configuration as well as the final relaxed configuration (conjugate gradient technique) at a 120° mildly-repulsive screw superdislocation intersection in $L1_2$ Ni_3Al, obtained using the Angelo potential for Ni_3Al [4]. The screw superdislocation had a $[1\,\bar{1}\,0]$ Burgers vector, $\langle 1\,\bar{1}\,0\rangle$ line direction and was introduced as two superpartials with each superpartial as two Shockley partials separated by $5b$ along the $[1\,1\,\bar{2}]$ direction on the $(1\,1\,1)$ glide plane. The center of the leading superpartial was displaced by $2a[1\,1\,\bar{2}]$ along the $[1\,1\,\bar{2}]$ direction on the $(1\,1\,1)$ glide plane. The intersecting dislocation had a Burgers vector of $[1\,0\,\bar{1}]$ and a line direction of $\langle 0\,\bar{1}\,\bar{1}\rangle$ and was introduced at the center of the simulation cell as two superpartials using its anisotropic elasticity displacement field. The glide plane of the intersecting dislocation was $(1\,\bar{1}\,1)$. The separation between the superpartials was obtained from 2-D atomistic simulations [4]. In the final relaxed configuration, it is seen that the screw superpartials have spontaneously cross-slipped onto the $(1\,1\,\bar{1})$ cross-slip plane on one side of the intersection forming a PPV-like [4] partially cross-slipped configuration at the intersection. Note, that both the leading and trailing screw superpartial dislocations have spontaneously cross-slipped at the intersection. This suggests that at the mildly repulsive intersection, formation of the PPV-like configuration is spontaneous and athermal with zero cross-slip activation energy in $L1_2$ Ni_3Al. The dislocation reactions at the intersection are very similar to the reactions obtained for the mildly-repulsive 120° intersection in FCC Ni.

4. Discussion

Current understanding of the FCC metal deformation describes three stages of deformation that are in a large part tied to dislocation micromechanisms, one of which is cross-slip [19–21]. However, the models and mechanisms for cross-slip remain quantitatively unresolved. Many models for cross-slip require high stresses that appear to be unrealistic when compared to the experimentally observed stresses under some conditions of profuse cross-slip [5]. One mechanism often invoked to provide a locally high stress is the ad hoc introduction of dislocation obstacles that leads to local stress fields that may be sufficient for cross-slip nucleation. Yet, profuse cross-slip (double-cross-slip multiplication and cross-slip annihilation) is known to occur even during Stage I deformation in ultrapure metals when the *extrinsic* obstacle hypothesis seems unreasonable. However, as this and the prior work shows, the dislocations themselves appear to provide important *intrinsic* obstacles for cross-slip nucleation that are heretofore insufficiently studied. Specifically, the present work shows that the activation energy for nucleation of cross-slip in an FCC metal containing a dislocation forest can be zero at selected mildly-repulsive dislocation intersections. As the visualizations in the present figures suggest, the reason for the radical drop in activation energy is clearly tied to the configurations and the interactions of the Shockley partial dislocations, themselves. The interactions at that scale have not been considered, defining such intersections as mildly repulsive as in the prior studies. Such configurations may intrinsically facilitate cross-slip for cutting the initially grown-in forest dislocations and continue through to enable profuse cross-slip under multi-slip during the later stage conditions. Further this work, along with previous calculations on mildly-attractive screw-dislocation intersections,

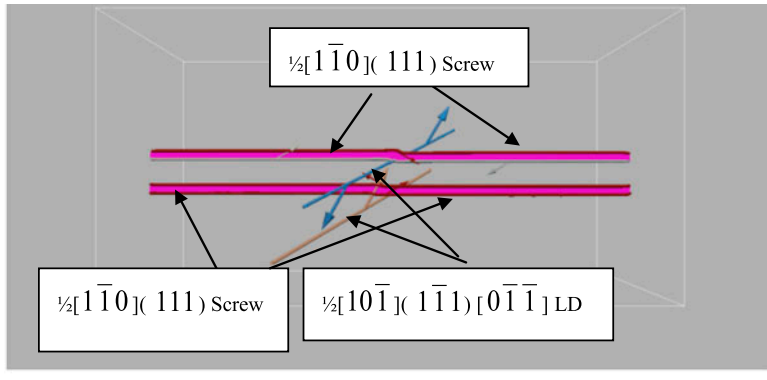

Initial

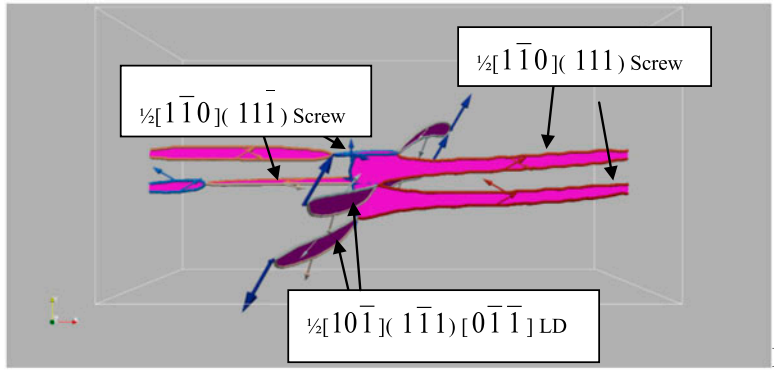

Final

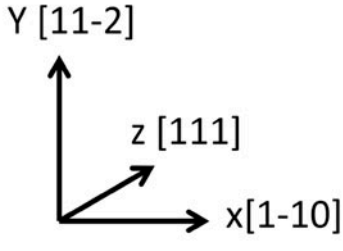

Figure 10. (colour online) A dislocation line representation of the initial and final relaxed atomic positions at a mildly repulsive 120° screw superdislocation intersection in $L1_2$ Ni_3Al obtained using the Angelo potential. Both the leading and trailing screw superpartials have partially cross-slipped to form a PPV like configuration.

provides a mechanism to obtain variations in the nucleation barrier for cross-slip with type of slip system interaction within a given system. Finally, these results suggest that cross-slip should preferentially nucleate at selected screw-dislocation intersections in $L1_2$ Ni_3Al.

One prior study by Washburn, has considered the role of dislocation intersections in the all-important dislocation multiplication processes occurring at low stresses in Stage I [22]. The study also considered intersection cross-slip for BCC and HCP metals.

According to Washburn, double intersection cross-slip, where a dislocation segment that has been pulled into the cross-slip plane soon encounters another intersection that brings it back onto another primary glide plane, which provides a reasonable mechanism for dislocation multiplication and for the growth of slip bands at low temperatures. However, the study by Washburn only considered attractive intersections (as in our prior work) and was unable to give quantitative analyses of the activation energies for such proposed mechanisms. Here, the unexpected finding is that even mildly-repulsive intersections lead to spontaneous cross-slip nucleation having zero activation energy. The finding provides strong motivation for a future more comprehensive study of repulsive intersections more generally. Any such studies should be extended to include an evaluation of the likelihood of occurrences of the myriad intersection types as a function of crystal orientation, deformation stage and sense of the applied stress.

On closing, we speculate on the merits of higher-level simulations that incorporate these new found mechanisms. We suggest that the results from this study, along with the results of our prior studies of cross slip at attractive intersections and at surfaces [1–4], [23], can be used for mesoscale dislocation ensemble simulations within the dislocation dynamics framework. Including such mechanisms in addition to the FE-mechanism model for cross-slip in isolation are likely to permit improved simulations of behaviours such as strain hardening and fatigue that have not been possible without ad hoc assumptions about obstacles for nucleating cross-slip at reasonable stresses. Such simulations are required to understand the relative importance of various cross-slip mechanisms, in isolation, attractive and repulsive intersection cross-slip, during various stages of deformation in the stress–strain curve of FCC crystals, including the onset of stage III deformation and to understand whether cross-slip is the controlling mechanism for the onset of stage III deformation. For example, within the present mechanism the frequency of intersection cross-slip nucleation is likely to scale with the forest dislocation density, i.e. the dislocation multiplication rate is proportional to ρ_f. The growth of such nuclei should depend upon the relative magnitudes of local stresses on the glide plane and the cross-slip plane at the partially cross-slipped screw-dislocation intersection region. Such behaviour of the partially cross-slipped core under different modes of applied stress could be studied using atomistic simulations as well as dislocation dynamics simulations.

Also, theories of Stage II single-crystal deformation in FCC metals that stem from the point-obstacle model of strain-hardening, assume that dislocation storage is a result of junction formation [24], or two-dimensional (2-D) concave loop formation [25] as the gliding dislocation traverses through an array of forest dislocation obstacles on its glide plane. However, one of the major problems in the point-pinning strain-hardening models is to explain how the generation of a 3-D network of stored dislocations occurs as a consequence of 2-D glide [25]. We note that the intersection cross-slip nucleation mechanism naturally provides a means for generating a 3-D network of dislocations from a 2-D glide.

5. Summary

(1) Screw dislocations are found to spontaneously cross-slip having zero activation energy at mildly-repulsive dislocation intersections in FCC Ni, Cu and $L1_2$

Ni_3Al. The direction of spontaneous cross-slip is postulated to be related to the strength of junctions formed at the intersection.

(2) The mechanism of spontaneous cross-slip of screw dislocations at mildly-repulsive intersections is analogous to the classical 'FE mechanism', wherein the necessary constriction formation is aided by the interaction forces from the intersecting dislocations at the Shockley partial level leading to a markedly reduced or a eliminated cross-slip activation energy. However, the exact mechanism in a particular material may depend upon the details of the atomic interactions.

(3) Given the spontaneous nature of cross-slip at mildly repulsive intersections and the much reduced energies at other intersections (prior work), together with the high likelihood of forest dislocations existing even in pure well annealed metal crystals, there are strong indications that extrinsic obstacles are not required to promote cross-slip and double cross-slip during deformation.

Acknowledgements

The authors acknowledge use of the 3d molecular dynamics code, LAMMPS, which was developed at Sandia National Laboratory by Dr Steve Plimpton and co-workers. This work was supported by AFOSR (Dr David Stargel), and by a grant of computer time from the DOD High Performance Computing Modernization Program, at the Aeronautical Systems Center/Major Shared Resource Center. The work was performed at the US Air Force Research Laboratory, Materials and Manufacturing Directorate, Wright–Patterson AFB. JAE acknowledges support by DARPA Grant # N66001-12-1-4229.

References

[1] S. Rao, D.M. Dimiduk, J. El-Awady, T.A. Parthasarathy, M.D. Uchic and C. Woodward, Phil. Mag. 89(34) (2009) p.3351.
[2] S. Rao, D.M. Dimiduk, J. El-Awady, T.A. Parthasarathy, M.D. Uchic and C. Woodward, Acta Mater. 58 (2010) p.5547.
[3] S. Rao, D.M. Dimiduk, T.A. Parthasarathy, J. El-Awady, M.D. Uchic and C. Woodward, Acta Mater. 59 (2011) p.7135.
[4] S.I. Rao, D.M. Dimiduk, T.A. Parthasarathy, M.D. Uchic and C. Woodward, Scripta Mater. 66 (2012) p.410.
[5] W. Püschl, Prog. Mater Sci. 47 (2002) p.415.
[6] P.J. Jackson, Prog. Mater Sci. 29 (1985) p.139.
[7] J. Bonneville and B. Escaig, Acta Metall. 27 (1979) p.1477.
[8] J. Bonneville, B. Escaig and J.L. Martin, Acta Metall. 36 (1988) p.1989.
[9] B. Escaig, *Proceedings of the Battelle colloquium on dislocation dynamics*, in A.R. Rosenfield, G.T. Hahn, A.L. Bement Jr., and R.I. Jaffee (New York: McGraw-Hill), 1968, p.655.
[10] D. Caillard and J.L. Martin, *Thermally Activated Mechanisms in Crystal Plasticity*, Pergamon-Elsevier, Amsterdam, 2003.
[11] G. Saada, Mater. Sci. and Engr A. 137 (1991) p.177.
[12] S.J. Plimpton, J. Comp. Phys. 117 (1995) p.1.
[13] J.E. Angelo, N.R. Moody and M.I. Baskes, Modell. Simul. Mater. Sci. Eng. 3 (1995) p.289.
[14] S. Rao, T.A. Parthasarathy and C. Woodward, Phil. Mag.A. 79 (1999) p.1167.
[15] Y. Mishin, Acta Mater. 52 (2004) p.1451.
[16] Y. Mishin, M.J. Mehl, D.A. Papaconstantopoulos, A.F. Voter and J.D. Kress, Phys. Rev. B 63 (2001) p.224106.

[17] A. Stukowski and K. Albe, Model. Simul. Mater. Sci. Eng. 18 (2010) p.085001.
[18] R.L. Fleischer, Acta Metall. 7 (1959) p.134.
[19] E. Nes and K. Marthinsen, Mater. Sci. Eng. A322 (2002) p.176.
[20] J. Gil Sevillano, in *Materials Science and Technology, A Comprehensive Treatment*, v6, R. W. Cahn, P. Haasen and E.J. Kramer, VCH, Weinheim, 1993, p.19.
[21] H. Mecking and U.F. Kocks, Acta Metall. 29 (1981) p.1865.
[22] J. Washburn, J. Appl. Phys. Letters 7 (1965) p.183.
[23] S. Rao, D.M. Dimiduk, T.A. Parthasarathy, M.D. Uchic and C. Woodward, Acta Mater. 61 (2013) p.2500.
[24] B. Devincre, T. Hoc and L. Kubin, Science 320 (2008) p.1745.
[25] U.F. Kocks and H. Mecking, Prog. Mater Sci. 48(3) (2003) p.102.